CrystEngComm

Accepted Manuscript

ROYAL SOCIETY OF CHEMISTRY

www.rsc.org/crystengcomm

The Nature of the C-Cl···Cl-C Intermolecular Interactions Found in Molecular Crystals. A General Theoretical-Database Study Covering the 2.75 – 4.0 Å Range

Marçal Capdevila-Cortada, Júlia Castelló, and Juan J. Novoa*

Departament de Química Física and IQTCUB, Facultat de Química, Universitat de Barcelona, Av. Diagonal 645, 08028 Barcelona (Spain)

E-mail: juan.novoa@ub.edu

ABSTRACT: The nature of C-Cl···Cl-C interactions in molecular crystals has been evaluated at the MP2/aug-cc-pVDZ computational level, after test computations on simple model systems showed that such computational level predicts for model dimers the same angular dependence and impact of the C(*ipso*) atom hybridization than MP2/CBS computations. Thus MP2/aug-cc-pVDZ calculations predict a C(sp^n)-Cl···Cl- C(sp^n) strength of -0.73, -0.87, and -0.96 kcal·mol^{-1} for n = 3, n = 2 (non-aromatic), and n = 1 (all BSSE-corrected values) at their most stable orientation, while for the same orientations and hybridization MP2/CBS calculations predict a value of -1.14, -1.29, and -1.40 kcal·mol^{-1}.

A first group of computations on model dimers allows to conclude that the strength of the C-Cl···Cl-C interactions depends on: (a) the number of short distance Cl···Cl contacts involved; (b) the hybridization of the C(*ipso*) atom [E(Csp^2) > E(Csp) > E(Csp^3)]; (c) the degree of chlorination of the C(*ipso*) atom; and (d) the relative orientation of the two C-Cl groups. Two types of minima were found in the E(θ_1, θ_2) potential energy surface [θ_1 = <C(1)-Cl(2)···Cl(3) and θ_2 = <Cl(2)···Cl(3)-C(4)]: Type I minima, where $\theta_1 = \theta_2 = 90^o$, and Type II minima, energetically more stable, where $\theta_1 = 180^o$ and $\theta_2 = 90^o$ or $\theta_1 = 90^o$ and $\theta_2 = 180^o$ (the orientation where $\theta_1 = \theta_2 = 155^o$ (a Type I geometry) is a saddle point in E(θ_1, θ_2) that connects the two Type II minima).

The interaction energy was also computed for 45 C-Cl···Cl-C containing dimers extracted from the Cambridge Crystallographic Data Centre (CCDC), and having a Cl···Cl distance smoothly distributed within the 2.75 – 4.0 Å range. The nature of these interactions was further characterized by looking at: (a) the dominant component of the dimer interaction energy; and (b) the characteristic properties of their only Cl···Cl bond critical point (evaluated from an Atoms-in-Molecules (AIM) analysis of the dimer electron density). Their interaction energy is dominated by the dispersion component, although a much weaker electrostatic component is also present for some cases. These interactions fail to fulfill the strength-length distribution that should correlate E_{int} and the Cl···Cl distance. A previously proposed correlation between the electron density at the Cl···Cl bond critical point and the strength of the C-Cl···Cl-C interaction is shown to fail for short Cl···Cl distances.

INTRODUCTION

Halogen···halogen (X···X) interactions have been a matter of interest and debate for many years.[1–8] Despite their weak strength, it is known that they are responsible for the packing and properties of many molecular crystals. These interactions, as well as other non-covalent interactions such as hydrogen bonds (*A*-H···*B*),[9–11] halogen bonds (*A*-X···*B*),[12,13] stacking interactions (π···π),[14–16] or non-classical hydrogen bonds (C-H···*B*),[17–19] are the tools for a rational design of molecular solids, i.e., they play an important role in crystal engineering.[20,21]

Over the past years, many studies have attempted to rationalize the nature of X···X interactions. On the one hand, these interactions were associated to specific attractive forces.[4,22] On the other hand, they were justified in terms of a non-spherical shape of the halogen charge density, which caused a decrease on the exchange-repulsion interaction.[23–25] Both models agree connect the strength of the X···X interactions with the electron density anisotropy, but whereas the former considered its nature attractive, the latter manifested a decrease on its repulsive character. This fact prompted several authors to focus their work in the analysis of X···X interactions charge density,[7,26,27] finding a correlation between the density topology and the strength.[26]

Analysis of the crystals deposited in the Cambridge crystallographic database revealed two preferred geometry orientations for X···X interactions.[4] Defined such angularity as a function of θ_1 and θ_2, respectively the C(1)-Cl(2)···Cl(3) and the Cl(2)···Cl(3)-C(4) angles in a C(1)-Cl(2)···Cl(3)-C(4) interaction, the two preferred orientations arise when: (a) $\theta_1 = \theta_2$ (Type I orientations, usually associated with inversion centers and symmetry planes) and when $\theta_i \approx 180^o$ and $\theta_j \approx 90^o$ (Type II orientations, usually associated with screw axis and glide planes). It has been shown that Type I orientations have a maximum of probability of presence around 150º. The existence of regions of high probability for Type I and Type II interactions has been taken as an indication of the anisotropic distribution of the electron density around the halogen atoms, the so-called σ-hole.[28]

Finally, it is also known that the strength of X···X interactions depends on the type of halogen atom, according to the following tendency:[6] I > Br > Cl > F. The hybridization of the carbon atom to which the halogen is bonded (the C(*ipso*) carbon) is also known to affect the strength of the interaction, which decreases in the following order:[6] sp^2 > sp > sp^3.

Aimed at getting a general understanding of the X···X interactions in molecular crystals, in the present work we carry out an exhaustive study of the C-Cl···Cl-C interactions. The work is, thus, an extension of a previous study that elucidated the nature of the C-F···F-C interactions in perfluorinated molecular crystals.[29] The study of the C-Cl···Cl-C interactions is structured in two parts. In the first part, the interaction energy of the C-Cl···Cl-C interactions is evaluated for various orientations of the $(CCl_4)_2$ dimer. Then, the C-Cl···Cl-C interaction energy was computed for all non-equivalent first nearest-neighbors in the CCl_4 molecular crystal. The influence of dipole moment, hybridization of the *ipso* carbon, and angular dependence is analyzed on chloro-substituted methane, ethylene, benzene, and acetylene. SAPT and AIM calculations were also done to get a deeper understanding of the nature of these C-Cl···Cl-C interactions. In the second, the strength and nature of the C-Cl···Cl-C interactions was evaluated in a set of 45 dimers extracted from the Cambridge crystallographic database. These dimers were selected to have Cl···Cl distances ranging from 2.75 to 4 Å, in a way that they cover the whole range of distances smoothly. The nature of these interactions was further characterized by looking at the dominant component of the interaction energy, as well as by evaluating the characteristic properties of their only Cl···Cl bond critical point (obtained by doing an Atoms-in-Molecules, AIM, analysis of the electron density of the dimer). The results obtained in the second part were compared with those from the first part, in order to compare their trends.

METHODOLOGY

All energy calculations were carried out at the MP2 level, using the aug-cc-pVDZ basis set. According to previous studies of halogen···halogen interactions, the MP2/aug-cc-pVDZ methodology gives reliable interaction energies.[29] Such conclusion was confirmed by comparing the MP2/aug-cc-pVDZ and MP2/CBS results for three different orientations of the BSSE-corrected interaction energy for the $(CH_3Cl)_2$, $(H_2CCHCl)_2$, and $(HCCCl)_2$ dimers (CBS stands for complete basis set; the values were estimated using the Helgaker extrapolation[30,31] and the aug-cc-pVXZ (X = D, T, Q, 5). Figure 1 plots, for the $(CH_3Cl)_2$, $(H_2CCHCl)_2$, and $(HCCCl)_2$ dimers, the BSSE-corrected E_{int} values obtained at the MP2/aug-cc-pVDZ and MP2/CBS levels for the (180,180), (180,90) and (90,90) orientations shown in Figure 1. While MP2/aug-cc-pVDZ calculations predict that C(sp^n)-Cl···Cl-C(sp^n) interactions have a strength of -0.73, -0.87 and -0.96 kcal·mol^{-1} for n = 3, n = 2 (non-aromatic), and n = 1 (all are BSSE-corrected values), MP2/CBS calculations predict s strength of -1.14 -1.29 and -1.40 kcal·mol^{-1}. Thus, the two computational levels predict the same relative stability of the C(sp^n)-Cl···Cl- C(sp^n) interactions of Figure 1, as well as for impact of the C(*ipso*) hybridization. Consequently, the aug-cc-pVDZ basis set will be used in the rest of this work, devoted to study variations of the C-Cl···Cl- C strength for various properties. Notice, in passing, that the MP2/CBS values reported before can be taken as benchmark results for the strength of C(sp^n)-Cl···Cl-C(sp^n) interactions, for n = 3, 2 (non-aromatic), and 1.

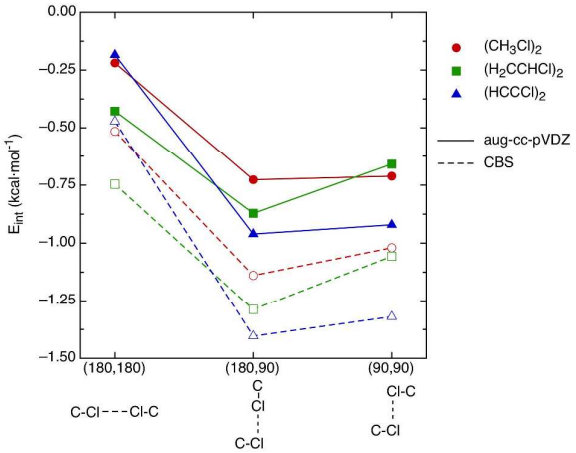

Figure 1. Plot of the variation with the orientation of the interaction energies of $(CH_3Cl)_2$, $(H_2CCHCl)_2$, and $(HCCCl)_2$ dimers computed at the MP2/aug-cc-pVDZ (BSSE-corrected values) and MP2/CBS levels. The orientations are shown under the plot.

All potential energy curves and 2D surfaces were obtained optimizing the remaining variables. All optimizations and interaction energy calculations were performed using the Gaussian03 package.[32] The Basis Set Superposition Error (BSSE) was always corrected, using the full counterpoise approach.[33]

The nature of the interaction energy was further characterized by doing Symmetry Adapted Perturbation Theory (SAPT) calculations,[34] a perturbative method where the interaction energy of two closed-shell fragments is decomposed into four components: the electrostatic (E_{el}), exchange-repulsion (E_{ex}), induction (E_{ind}), and dispersion (E_{disp}) components, as specified in the literature.[29,35]

$$E_{\text{int}} = E_{el} + E_{ex} + E_{ind} + E_{disp} \quad (1)$$

The SAPT2 level of the SAPT algorithm, which is roughly equivalent to second-order MP2 calculations, was employed. All SAPT calculations were done with the SAPT2008 program.[36]

Intermolecular bonds were characterized by means of the Atoms-In-Molecules (AIM) methodology,[37] using an in-house version of the PROAIM program.[38] In the AIM methodology any intermolecular bond is associated with a (3,-1) bond critical point (BCP), i.e., a point in the electron density surface where the gradient of the density is zero and its second derivative has two negative and one positive eigenvalues (a (3,-1) signature). Each BCP is characterized by its density and Laplacian (the sum of the curvatures of the density at the BCP).

Searches for C-Cl···Cl-C intermolecular interactions on published molecular crystals were performed on the Cambridge Crystallographic Data Centre (CCDC),[39] using the 5.35, November 2013 version. The following filters were applied: 3D coordinates determined, not disordered, no errors, not polymeric, no powder structures, and a crystallographic R factor ≤ 0.05. The search was limited to Cl···Cl distances within the 2.75 – 4 Å range. In order to facilitate the analysis of the results, these results are only presented for those crystal dimers showing only one Cl···Cl bond critical point.

RESULTS AND DISCUSSION

1. Cl···Cl Interactions in Perchloromethane.

The study of the directionality and strength of the Cl···Cl interactions begun with an in-depth analysis of prototypical orientations of the $(CCl_4)_2$ dimer. This dimer was selected because it allows the study of purely dispersive C-Cl···Cl-C interactions (both interacting fragments have neither a net charge, nor a net dipole moment, and thus the electrostatic component should be very small or negligible). Six representative orientations of the $(CCl_4)_2$ dimer were considered (see Figure 2). The interaction energy curves for all six orientations (Figure 3) reveal the higher stability of the (3:3 sta) dimer, whose E_{int} is 2 kcal·mol^{-1} more stable than that for any other curve (following in stability are the (2:1), (3:1), and (3:3 ecl) orientations). Such relative stability is related to the number of intermolecular bonds present in each orientation (obtained from an AIM analysis), also plotted in Figure 2. The (3:3 sta) dimer presents six intermolecular bonds (i.e., six BCP), while (3:3 ecl) and (3:1) exhibit three intermolecular bonds and the (2:1) orientation presents only one. It is worth pointing the higher stability of the (2:1) orientation respect to the (2:2), which also shows two intermolecular bonds. This fact suggests the impact of directionality on the strength of the C-Cl···Cl-C interactions, a point investigated in detail in the following section.

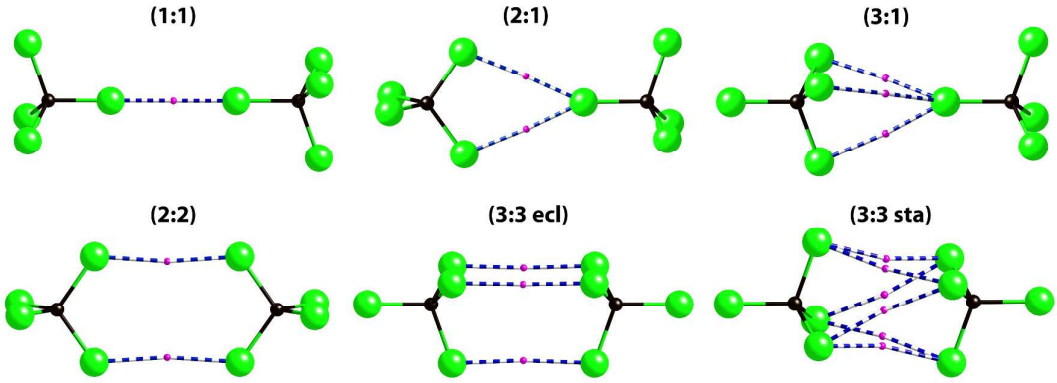

Figure 2. The six orientations considered of the $(CCl_4)_2$ dimer. The bond critical points at their equilibrium distance resulting from an AIM analysis of the wavefunction (obtained at the MP2/aug-cc-pVDZ level) are also shown.

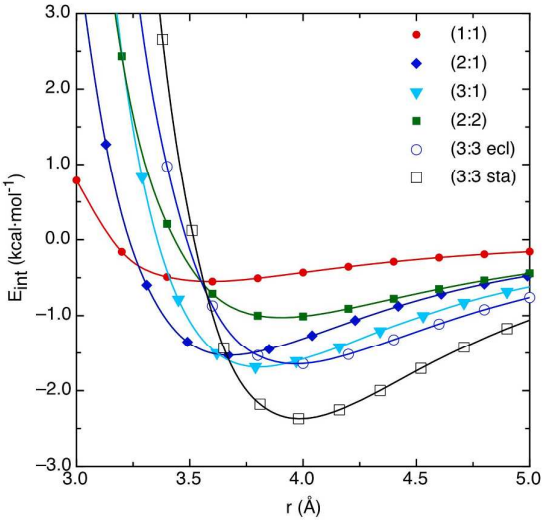

Figure 3. Interaction energy curves obtained at the MP2/aug-cc-pVDZ level, for the six $(CCl_4)_2$ models of Figure 1. The BSSE is corrected. The parameter *r* is defined as the shortest Cl···Cl distance.

The results obtained for the six $(CCl_4)_2$ model dimers in Figure 2 were compared with the interaction energy for all symmetry-unique first-nearest-neighbor dimers present in the CCl_4 molecular crystal (Figure 4, Refcode: CARBTC), all presenting C-Cl···Cl-C interactions. There are seven non-equivalent first-nearest-neighbor dimers in this crystal, all having a Cl···Cl distance smaller than 4 Å. In the following, these dimers are identified as the **A-G** dimers, see Figure 5). Dimers **C**, **E**, and **F** are almost identical to the (2:1) model dimer of Figure 2, while dimer **B** is a (1:1) orientation. On the other hand, dimer **A** is a parallel-displaced (2:2) dimer, and dimer **G** is close to the (3:3 sta) dimer of Figure 2. However, dimer **D** is a (3:2) type not considered before. According to these similarities, dimer **G** should be the most stable one, while dimer **B** should be the least stable. The computed interaction energy of the **A-G** dimers (Table 1) is in good agreement with these estimations: **G** is the most stable dimer (2 kcal·mol^{-1} more stable than the **D** dimer), followed in stability by the **A**, **C**, **E**, and **F** dimers, while **B** is the least stable dimer (E_{int} of -0.9 kcal·mol^{-1}).

In order to get a deeper insight on the nature of the C-Cl···Cl-C interactions, one can look at the components of the interaction energy, obtained by doing SAPT calculations on the (1:1) orientation of the $(CCl_4)_2$ dimer (first row in Table 2). The SAPT total interaction energy (-0.5 kcal·mol^{-1}) is the same than the MP2 value (fact that can be taken as a confirmation of the validity of the SAPT decomposition). The dominant component is the dispersion term. It is also worth mention the non-negligible size of the electrostatic component, repulsive in character, which can only be caused by the partial charge on the chlorine atoms, probably enhanced by the already mentioned anisotropy of the density around the Cl atom.[28]

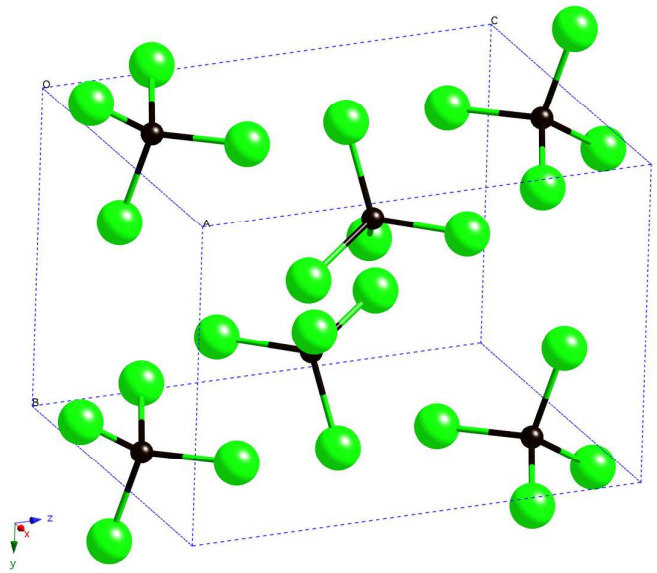

Figure 4. Unit cell of the CCl_4 crystal (CCDB Refcode: CARBTC).

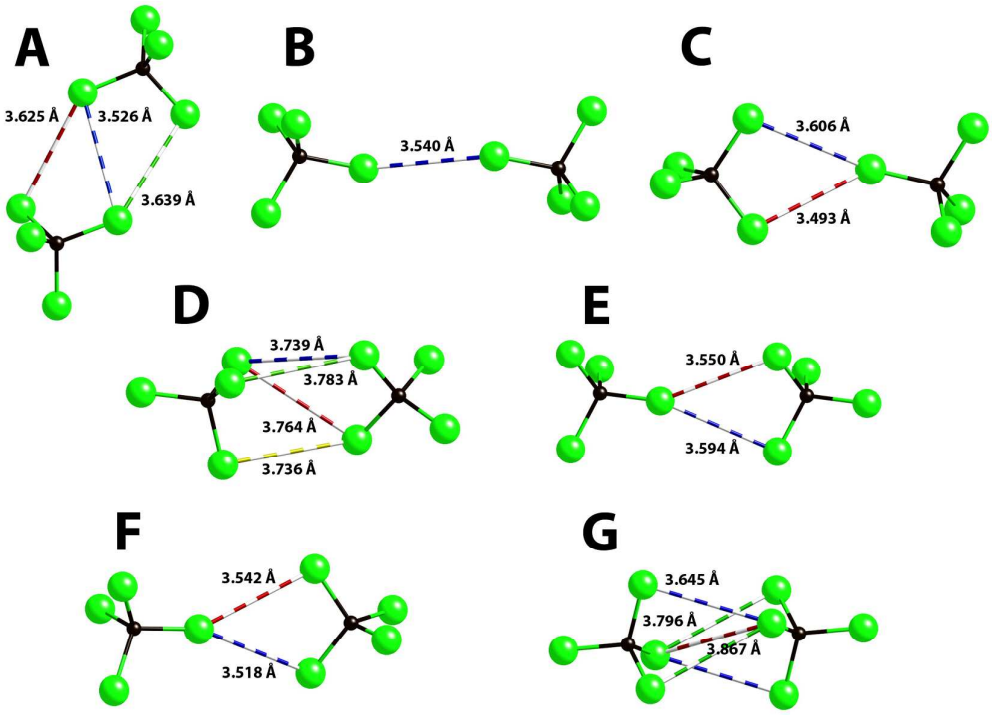

Figure 5. Orientation of the seven non-equivalent dimers present in the CCl_4 crystal. All Cl···Cl interactions shorter than 4.0 Å are shown in dashed lines.

Table 1. Interaction energy of the seven non-equivalent dimers present in the CCl_4 crystal (Figure 5). Calculations done at MP2/aug-cc-pVDZ level, BSSE corrected. The density and Laplacian of all BCPs of each dimer are also shown.

dimer	contact	E_{int} (kcal·mol^{-1})	r (Å)	ρ (a.u.)	∇^2 ρ (a.u.)
A	~(2:2)	-1.40	3.63	$3.7\cdot10^{-3}$	0.015
			3.53	$7.6\cdot10^{-3}$	0.025
			3.64	$6.4\cdot10^{-3}$	0.020
B	(1:1)	-0.94	3.54	$9.1\cdot10^{-3}$	0.011
C	(2:1)	-1.17	3.61	$5.0\cdot10^{-3}$	0.016
			3.49	$8.0\cdot10^{-3}$	0.024
D	(3:2)	-1.72	3.74	$6.9\cdot10^{-3}$	0.014
			3.78	$4.3\cdot10^{-3}$	0.013
			3.76	$7.3\cdot10^{-3}$	0.014
			3.74	$6.3\cdot10^{-3}$	0.015
E	(2:1)	-1.43	3.55	0.011	0.017
			3.59	0.010	0.019
F	(2:1)	-1.37	3.54	$9.3\cdot10^{-3}$	0.023
			3.52	$8.9\cdot10^{-3}$	0.024
G	~(3:3 sta)	-2.15	3.65	$5.8\cdot10^{-3}$	0.020
			3.65	$5.8\cdot10^{-3}$	0.020
			3.80	$4.4\cdot10^{-3}$	0.015
			3.80	$4.4\cdot10^{-3}$	0.015
			3.87	$4.1\cdot10^{-3}$	0.013

2. Impact of the Degree of Chlorination in the C(*ipso*) carbon.

As already mentioned, due to its symmetry, the CCl_4 molecule has no net dipole moment. However, when the chlorination degree is decreased from 4 to a value of 1, as that found in the CH_3Cl molecule, a dipole moment is created in the new molecule. This dipole moment induces the presence of an electrostatic component in the C-Cl ···Cl-C interaction energy.

The importance of the electrostatic component in the interaction energy was tested in the $(CH_3Cl)_2$, $(CH_2Cl_2)_2$ $(CHCl_3)_2$, and $(CCl_4)_2$ dimers (see Table 2, which collects for each dimer, its optimum distance, dipole moment, and interaction energy). All dimers were oriented as the (1:1) dimer, that is, with $\theta_1 = \theta_2 = 180°$ (see Figure 2). Although there is an increase in the dipole moment of each interacting fragment when the chlorination degree is decreased, the interaction energy does not present a clear trend. The $(CHCl_3)_2$ dimer has the largest interaction energy, being slightly more stable than the $(CH_2Cl_2)_2$ and $(CCl_4)_2$ dimers.

In order to find the reasons of such a trend, an SAPT analysis of the components of the interactions energy was carried out (Table 2). The E_{ex}, E_{ind}, and E_{disp} components decrease with the chlorination degree (in absolute value), a trend mostly associated to the change in the dimer Cl···Cl distance. However, the electrostatic term follows a different trend with the degree of chlorination, due to the change in the relative orientation of the dipole moments of each molecule of the dimer (Figure 6). Thus, while in the $(CHCl_3)_2$ and $(CH_2Cl_2)_2$ dimers the orientation of the dipole moments is stabilizing (negative E_{el} term), in the $(CH_3Cl)_2$ dimer the interaction is destabilizing (positive E_{el} term). Once again, note the close values of E_{int} obtained using the SAPT and MP2 methods, thus confirming the reliability of the SAPT decomposition.

Table 2. Interaction energy (MP2) and SAPT decomposition of the $(CCl_4)_2$, $(CHCl_3)_2$, $(CH_2Cl_2)_2$, and $(CH_3Cl)_2$ dimers on their (1:1) orientation. The aug-cc-pVDZ basis set was used and the BSSE was corrected. All energy values are given in kcal·mol^{-1}. Equilibrium Cl···Cl distance and dipole moment of each isolated monomer are also indicated.

	r (Å)	μ (D)	E_{el}	E_{ex}	E_{ind}	E_{disp}	$E_{int,SAPT}$	$E_{int,MP2}$
$(CCl_4)_2$	3.40	0.0	0.19	1.32	-0.28	-1.78	-0.54	-0.49
$(CHCl_3)_2$	3.43	1.28	-0.03	1.25	-0.21	-1.61	-0.59	-0.55
$(CH_2Cl_2)_2$	3.49	1.93	-0.10	1.10	-0.15	-1.41	-0.57	-0.53
$(CH_3Cl)_2$	3.55	2.18	0.17	0.94	-0.13	-1.23	-0.25	-0.22

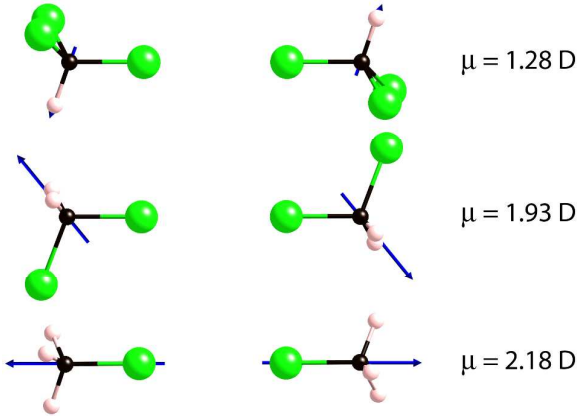

Figure 6. Relative orientation of the dipole moment in each molecule for the $(CHCl_3)_2$, $(CH_2Cl_2)_2$, and $(CH_3Cl)_2$ dimers.

The correlation between the interaction energy and the dipole moment is also manifested when the angular dependence of the C-Cl···Cl-C interactions is analyzed. Figure 7 plots the $E(\theta_1, \theta_2)$ potential energy surface of the $(CH_3Cl)_2$ dimer (that is, as a function of the θ_1 and θ_2 angles). In good agreement with the results from previous crystallographic studies,[4] two types of minima are observed: Type I minima, when $\theta_1 = \theta_2 = 90º$, and Type II minima when $\theta_1 = 180º$ and $\theta_2 = 90º$, or when $\theta_2 = 180º$ and $\theta_1 = 90º$. Also shown in Figure 7, is the facts that Type I orientations (i.e., those where $\theta_1 = \theta_2$) presents a maximum around 120º and a metastable minimum when $\theta_1 = \theta_2 = 155º$. In the $E(\theta_1, \theta_2)$ potential energy surface the latter point is a saddle point connecting both Type II minima. These results suggest that Type I minima should be restricted to some θ ranges, as suggested in previous studies.[6]

A SAPT analysis of the components of the interaction energy was also carried out at of (90,90), (90,180), (180,90), and (180,180), orientations of Figure 7. As shown in Table 3 (first row of each subset), dispersion is the dominant component of the interaction energy. It is also relevant the fact that the larger stabilization of the (90,90), (90,180) and (180,90) orientations respect to the (180,180) configuration is mostly due to changes in the electrostatic component.

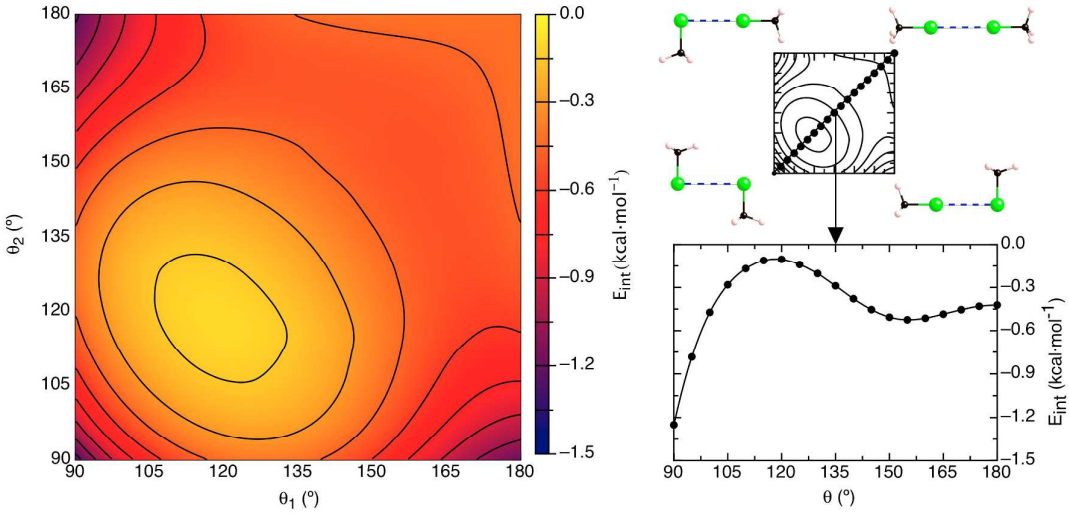

Figure 7. Interaction energy surface on the θ_1 and θ_2 angles for the $(CH_3Cl)_2$ dimer, obtained at MP2/aug-cc-pVDZ level. The BSSE was not corrected. The interaction energy profile for Type I interactions ($\theta_1 = \theta_2$) is also shown.

3. Impact of the C(*ipso*) Hybridization.

The impact of the C(*ipso*) hybridization was analyzed by doing a SAPT analysis of the interaction energy of the $(H_2CCHCl)_2$, $(C_6H_5Cl)_2$, and $(HCCCl)_2$ dimers. These dimers were oriented in such a way that they presented a C-Cl···Cl-C interaction at their (180,180), (180,90), (90,180) and (90,90) geometry (see Figure 7, due to the dimer symmetry, the energy of the (90,180) and (180,90) is the same and, consequently, only one is shown). These results, together with those already described on the $(H_3CCl)_2$ dimer, allows us to evaluate the impact on the C-Cl···Cl-C strength of the C(*ipso*) hybridization, for C(sp^3), C(sp^2(aliphatic)), C(sp^2(aromatic)), and C(sp).

Table 3 collects the SAPT analysis for the interaction energy of each dimer, together with their interaction energy. Note also here the similarity between the MP2 and SAPT interaction energies. In all dimers and geometries the dispersion component is the dominant stabilizing component of the interaction energy. The $(C_6H_5Cl)_2$ dimer is the most stable dimer at all orientations. Interestingly, the $(C_6H_5Cl)_2$ is more stable than the $(H_2CCHCl)_2$ dimer, thus pointing to relevant aromatic effects. The remaining dimers have similar interaction energies.

The existence of anisotropy effects is reflected in: (a) the change in the electrostatic, dispersion, and exchange-repulsion components when going from the (180,180) orientation to the (180,90) and (90,90) orientations, similar in the three hybridizations, and (b) the change in the electrostatic term of the $(HCCCl)_2$ dimer from being repulsive at the (180,180) orientation, to attractive at the (90,90) orientation. The directionality is similar for all hybridizations.

Table 3. Interaction energy (MP2) and SAPT decomposition of the $(CH_3Cl)_2$, $(H_2CCHCl)_2$, $(C_6H_5Cl)_2$, and $(HCCCl)_2$ dimers on three (θ_1, θ_2) orientations. The BSSE was corrected. All energy values are given in kcal·mol^{-1}. Their equilibrium Cl···Cl distance is also indicated. The aug-cc-pVDZ basis set was used in the MP2 calculations of all dimers and in the SAPT analysis of the $(CH_3Cl)_2$ and $(HCCCl)_2$ dimers, while in the SAPT calculation of the $(C_6H_5Cl)_2$ dimer (values in italics) the aug-cc-pVDZ was used for the Cl atoms and the cc-pVDZ for the C and H atoms.

	r (Å)	E_{el}	E_{ex}	E_{ind}	E_{disp}	$E_{int,SAPT}$	$E_{int,MP2}$
(180,180)							
$(CH_3Cl)_2$	3.55	0.17	0.94	-0.13	-1.23	-0.25	-0.22
$(H_2CCHCl)_2$	3.48	-0.05	1.14	-0.14	-1.42	-0.47	-0.43
$(C_6H_5Cl)_2$	3.41	*-0.11*	*1.49*	*-0.19*	*-1.66*	*-0.47*	-0.57
$(HCCCl)_2$	3.50	0.45	0.73	-0.17	-1.24	-0.22	-0.18
(180,90)							
$(CH_3Cl)_2$	3.47	-0.99	2.40	-0.33	-1.86	-0.77	-0.73
$(H_2CCHCl)_2$	3.46	-0.90	2.35	-0.30	-2.09	-0.94	-0.87
$(C_6H_5Cl)_2$	3.34	*-1.24*	*3.45*	*-0.44*	*-2.78*	*-1.01*	-1.28
$(HCCCl)_2$	3.42	-0.84	2.09	-0.32	-1.97	-1.03	-0.96
(90,90)							
$(CH_3Cl)_2$	3.82	-0.55	1.37	-0.17	-1.40	-0.76	-0.71
$(H_2CCHCl)_2$	3.69	-0.42	1.80	-0.17	-1.95	-0.73	-0.66
$(C_6H_5Cl)_2$	3.54	*-0.73*	*2.90*	*-0.26*	*-2.80*	*-0.90*	-1.25
$(HCCCl)_2$	3.62	-0.84	1.85	-0.13	-1.88	-0.99	-0.92

4. The Nature of C-Cl···Cl-C Interactions found in Molecular Crystals.

Up to this point, the properties of the C-Cl···Cl-C interactions have been explored on model dimers. In this section, the knowledge so far acquired using these model dimers will be generalized. For such a task, a systematic study of the C-Cl···Cl-C interactions will be done on dimers extracted from the molecular crystals deposited in the CCDC.

A search was carried out in the CCDC, looking for molecular crystals presenting C-Cl···Cl-C interactions and having a Cl···Cl distance placed within the 2.75 – 4 Å range (see Methodological details). There are 19540 non-equivalent contacts within such a range of distances, located in 8296 crystals. These contacts involve the following C(*ipso*) atom hybridizations: 8885 contacts correspond to C(sp^3) atoms, 10653 to C(sp^2) atoms (10402 of them, involving aromatic sp^2 carbons), and only 2 contacts correspond to C(sp) atoms, that is, nearly 99% of these contacts correspond to C(sp^3) and C(sp^2-aromatic) atoms. Their distribution with the Cl···Cl distance and θ_1 and θ_2 angles is shown in Figure 8. The distance histogram exhibits a maximum around 3.8 Å (0.3 Å, slightly longer than twice the van der Waals radius of a chlorine atom, 1.75 Å). The angles scattergram (here restricted to contacts with $r_{Cl\cdots Cl} < 3.5$ Å) shows a clear preference for Type I and Type II orientations. Type I orientations are more likely in the 130-170º region and around 90º, while there are no Type I interactions around 100º. It is worth pointing that this distribution qualitatively matches the shape of the E(θ_1, θ_2) potential energy surface (Figure 7). Furthermore, the minimum energy path that links both Type II orientations in Figure 7, also matches the results in Figure 8.

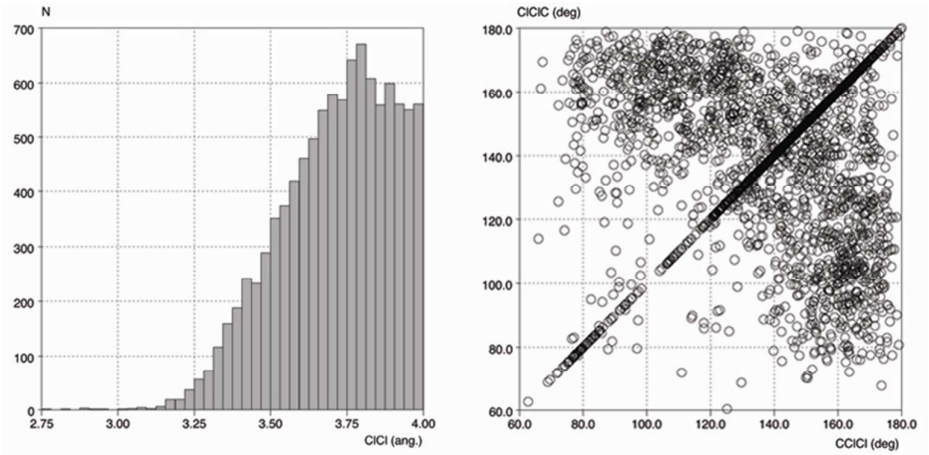

Figure 8. *Left*: Histogram plotting the number of Cl···Cl contacts as a function of the distance; *Right*: Scattergram showing the number of contacts as a function of the θ_1 and θ_2 angles, for contacts whose $r_{Cl\cdots Cl} < 3.5$ Å. These results were obtained by searching the Cambridge crystallographic database (CCDC).

Among all the dimers of the CCDC presenting C-Cl···Cl-C contacts with a Cl···Cl distance within the 2.75 – 4 Å, 45 dimers were selected for their computational study. These dimers were selected in such a way that their Cl···Cl distance spreads over the 2.75 – 4 Å range in a smooth way, while also cover the widest range of θ_1 and θ_2 angles and C(*ipso*) hybridization. Table 4 collects, for each of the 45 dimers, the Refcode of the crystal where they are found, the main geometric parameters, the interaction energy, and the characteristic properties of the Cl···Cl bond critical point (BCP; note that only dimers interactions presenting one Cl···Cl BCP were included in Table 4, a behavior confirmed after doing the AIM analysis). Figure 9 plots the variation of the interaction energy with the Cl···Cl distance (Figure 9, left) and with the θ_1 and θ_2 angles (Figure 9, right). The interaction energy increases with the Cl···Cl distance, reaching a maximum around 3.6 Å. In general, C-Cl···Cl-C interactions involving C(sp^2) atoms are slightly stronger than these involving C(sp^3) atoms (the sample on C(sp) interactions is not enough large allow us general conclusions). The angular dependence on the interaction energy follows the same potential energy surface computed in the $(CH_3Cl)_2$ dimer (Figure 7) and shows a clear preference for the regions where Figure 7 minima are placed (θ_1 = θ_2 = 90º Type I interactions, and the two Type II minima, which in the crystal dimers are not necessarily two equivalent minima). The data in Figure 10 also demonstrate the failure of the strength-length correlation (that is, the interaction energy and the distance are correlated in such a way that C-Cl···Cl-C interactions presenting a shorter Cl···Cl interfragment distance are more stable, thus having a more negative interaction energy), a failure already recognized in hydrogen bond interactions.[40] Such failure indicates that the Cl···Cl distance is not the only relevant parameter in defining the strength of the C-Cl···Cl-C interactions, that is, manifests the relevance of anisotropy in these interactions (see above).

Table 4. BSSE-corrected Interaction energy computed at the MP2/aug-cc-pVDZ level (in kcal·mol^{-1}) for the 45 dimers extracted from the CCDC, all presenting Cl···Cl distances within the 2.75 – 4 Å range. The Refcode of the crystal where they are present is also given), together with the Cl···Cl distance (in Å), the θ_1 and θ_2 angles (in degrees), and hybridization of the *ipso* carbon. Also given are the density (in a.u.), Laplacian (in a.u.), and local electronic kinetic energy density (in a.u.) of the Cl···Cl bond critical point, obtained from an AIM analysis of the dimer wavefunction.

Refcode	r	θ_1	θ_2	C(*ipso*) hyb.	ρ	$\nabla^2\rho$	G	E_{int}
CMALAM10	3.10	165.2	165.2	sp^3	0.011	0.046	$9.4\cdot10^{-3}$	-0.31
FEQYIK	3.14	164.2	164.2	sp^2	0.010	0.042	$8.7\cdot10^{-3}$	-0.07
EMILOB	3.18	160.7	160.7	sp^2	0.011	0.045	$9.0\cdot10^{-3}$	-1.01
DUZSIA	3.22	161.5	161.5	sp^3	$9.3\cdot10^{-3}$	0.035	$7.3\cdot10^{-3}$	-1.13
FOWBEY	3.23	156.5	156.5	sp^2	$9.1\cdot10^{-3}$	0.035	$7.2\cdot10^{-3}$	-0.51
AHUMUL	3.27	150.5	135.0	sp^2	$9.8\cdot10^{-3}$	0.035	$7.2\cdot10^{-3}$	-0.26
JOFJUK	3.27	154.2	154.2	sp^2	$8.8\cdot10^{-3}$	0.033	$6.3\cdot10^{-3}$	-0.25
IMIPOJ	3.28	158.7	158.7	sp^2	$8.3\cdot10^{-3}$	0.032	$6.5\cdot10^{-3}$	-0.88
HOFHEQ	3.29	155.8	155.8	sp^2	$8.4\cdot10^{-3}$	0.032	$6.5\cdot10^{-3}$	-0.70
CCINAM01	3.32	168.4	168.4	sp^2	$7.3\cdot10^{-3}$	0.029	$5.8\cdot10^{-3}$	-0.58
DCHLAN01	3.32	156.1	164.6	sp^2	$7.6\cdot10^{-3}$	0.029	$5.8\cdot10^{-3}$	-0.62
IFULUQ01	3.32	137.6	146.3	sp^2	$8.7\cdot10^{-3}$	0.031	$6.4\cdot10^{-3}$	-0.79
RIGVIN	3.33	96.5	159.8	sp^2	$9.0\cdot10^{-3}$	0.031	$6.6\cdot10^{-3}$	-2.23
DCLDXN03	3.37	156.9	156.9	sp^3	$7.5\cdot10^{-3}$	0.027	$5.5\cdot10^{-3}$	-0.49
UXIYOQ02	3.39	114.2	163.8	sp^3	$9.2\cdot10^{-3}$	0.031	$6.2\cdot10^{-3}$	-1.66
BAGCET [a]	3.39	104.4	164.4	sp^2	$7.2\cdot10^{-3}$	0.026	$5.3\cdot10^{-3}$	-1.52
DCLETH02	3.39	157.0	157.0	sp^3	$6.9\cdot10^{-3}$	0.025	$5.1\cdot10^{-3}$	-0.63
FOBTAS	3.40	160.9	160.9	sp^3	$6.4\cdot10^{-3}$	0.024	$4.8\cdot10^{-3}$	-0.75
PANFOB	3.43	111.5	166.2	sp^2	$8.1\cdot10^{-3}$	0.024	$5.1\cdot10^{-3}$	-1.22
OBUDIA	3.44	168.5	121.7	sp^2	$6.4\cdot10^{-3}$	0.023	$4.8\cdot10^{-3}$	-0.80
CLBZAP02	3.44	167.4	167.4	sp^2	$5.7\cdot10^{-3}$	0.022	$4.4\cdot10^{-3}$	-0.73
IDEKAE	3.47	151.7	151.7	sp^3	$6.1\cdot10^{-3}$	0.022	$4.4\cdot10^{-3}$	-0.25
SIFXEL	3.48	113.3	158.8	sp^2	$6.8\cdot10^{-3}$	0.022	$4.6\cdot10^{-3}$	-1.09
HAWXUY	3.48	175.8	103.7	sp^2	$6.6\cdot10^{-3}$	0.022	$4.6\cdot10^{-3}$	-1.70
DIRNOH	3.48	89.9	168.0	sp^2	$6.8\cdot10^{-3}$	0.023	$4.7\cdot10^{-3}$	-1.28
CIMALI	3.49	158.2	157.9	sp^3	$5.5\cdot10^{-3}$	0.020	$4.0\cdot10^{-3}$	-0.71
CCLACN	3.50	136.1	161.9	sp^3	$6.1\cdot10^{-3}$	0.020	$4.2\cdot10^{-3}$	-1.02
JADLIJ	3.53	145.3	145.3	sp^2	$5.8\cdot10^{-3}$	0.019	$4.0\cdot10^{-3}$	-0.92
CUKBUF01	3.54	91.4	176.5	sp^2	$6.1\cdot10^{-3}$	0.020	$4.2\cdot10^{-3}$	-2.33
ASOKUO	3.55	83.6	83.6	sp^3	$8.0\cdot10^{-3}$	0.023	$4.9\cdot10^{-3}$	-3.34
CLACET01	3.55	165.8	81.5	sp^3	$6.1\cdot10^{-3}$	0.020	$4.2\cdot10^{-3}$	-1.33
CORDUI	3.60	80.5	80.5	sp^3	$7.1\cdot10^{-3}$	0.021	$4.5\cdot10^{-3}$	-2.29
AJAHUO	3.62	142.8	142.8	sp^2	$4.9\cdot10^{-3}$	0.016	$3.3\cdot10^{-3}$	-1.15
FUGVAE	3.65	141.4	126.8	sp^2	$5.0\cdot10^{-3}$	0.016	$3.2\cdot10^{-3}$	-1.31
ADALUN	3.66	137.1	137.1	sp^2	$5.0\cdot10^{-3}$	0.015	$3.2\cdot10^{-3}$	-0.77
CLACET01	3.71	79.6	160.8	sp^3	$4.7\cdot10^{-3}$	0.014	$3.1\cdot10^{-3}$	-1.12
DAWSAV	3.71	91.6	91.6	sp^2	$5.8\cdot10^{-3}$	0.016	$3.5\cdot10^{-3}$	-2.18
CPXACA	3.73	133.5	133.5	sp^2	$4.6\cdot10^{-3}$	0.014	$2.9\cdot10^{-3}$	-0.66
CLACAM03	3.73	130.3	130.3	sp^3	$4.7\cdot10^{-3}$	0.014	$2.9\cdot10^{-3}$	-0.44
DCLNAQ	3.74	125.9	125.9	sp^2	$4.9\cdot10^{-3}$	0.014	$3.0\cdot10^{-3}$	-1.65
CCACEN	3.83	72.2	72.2	sp	$4.3\cdot10^{-3}$	0.013	$2.9\cdot10^{-3}$	-1.43
CLBECN03	3.84	115.4	115.4	sp^2	$4.3\cdot10^{-3}$	0.012	$2.5\cdot10^{-3}$	-0.59
CECPAB01	3.90	150.8	150.8	sp^2	$2.9\cdot10^{-3}$	$8.7\cdot10^{-3}$	$1.8\cdot10^{-3}$	-0.99
AMCLPY	3.93	132.4	132.4	sp^2	$3.2\cdot10^{-3}$	$9.1\cdot10^{-3}$	$1.9\cdot10^{-3}$	-0.58

[a] The 6-311+G(d) was used on the iodine atoms.

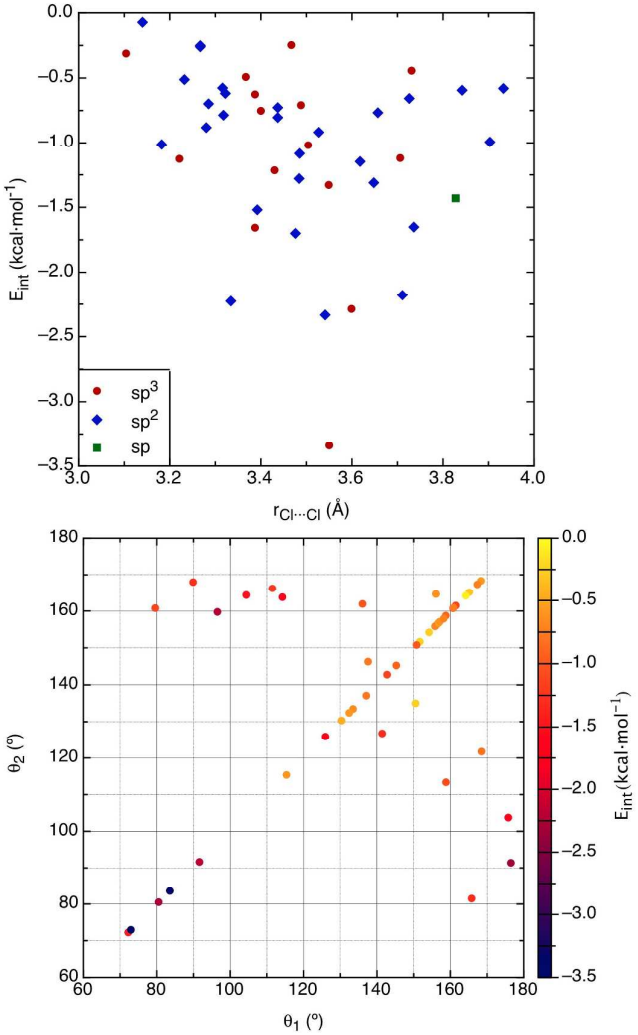

Figure 9. Variation of the interaction energy of the 45 dimers of Table 4 with the Cl···Cl distance (top) and with the θ_i angles (bottom). All energies were obtained at the MP2/aug-cc-pVDZ level and are BSSE-corrected. The values in the distance plot are grouped according to the C(*ipso*) hybridization.

The properties of the only Cl···Cl bond critical point present in the 45 dimers of Table 4 were also investigated (by doing Atoms-in-Molecules analysis of the dimer density) looking for the presence of correlations like those reported for hydrogen bonds.[41] The results of the AIM analysis are collected in Table 4. Figure 10 plots the variation of these properties (more specifically, of the density (ρ), Laplacian ($\nabla^2\rho$), and local kinetic energy density (G) at the bond critical point) as a function of the Cl···Cl distance (as already mentioned, only dimers presenting one Cl···Cl bond critical point were selected). As expected, the value of these properties decrease with the distance, in good agreement with reports for other intermolecular interactions.[26,29,42]

The validity of a previously reported correlation between the local electronic kinetic energy density at the bond critical point (G) and the dimer interaction energy[26] was also explored (these two properties were found to satisfy the expression $E_{int,G} = -0.429$ G). Figure 10 compares, for all dimers contained in Table 4, the interaction energy obtained using this equation and their MP2/aug-cc-pVDZ BSSE-corrected interaction energy. Clearly the proposed equation fails at short distances, although it provides acceptable interaction energies for distances around twice the van der Waals radius of chlorine.

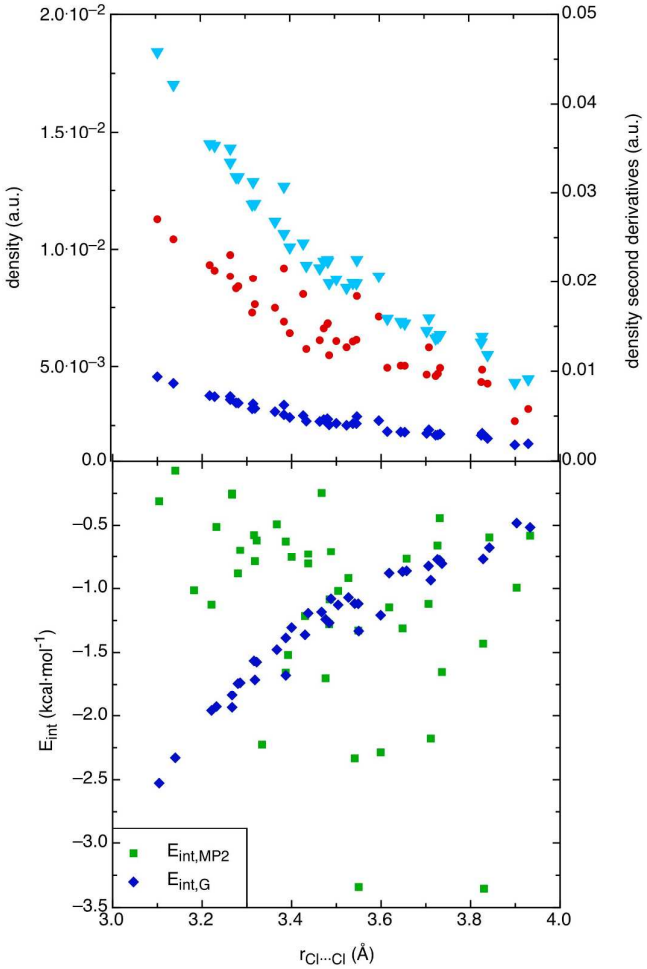

Figure 10. *Top:* Variation with the Cl···Cl distance of the characteristic properties of the Cl···Cl bond critical points reported in Table 4. Density (ρ) is shown in red circles (left axis), Laplacian (∇^2 ρ) is shown in light blue triangles (right axis), and local electronic kinetic energy density (G) is shown in dark blue rhombuses (right axis). *Bottom:* Comparison of the BSSE-corrected interaction energy obtained from MP2/aug-cc-pVDZ calculations ($E_{int,MP2}$) and by applying the $E_{int,G}$ = -0.429 G equation to the results of the AIM analysis,[26] ($E_{int,G}$).

Finally, amongst the 45 dimers collected in Table 4, 9 dimers were chosen for an evaluation of the components of the interaction energy (they were selected by systematically picking one-out-of-every-five dimers). For many selected dimers, limitations of the SAPT2008 package made impossible to perform an SAPT analysis of the interaction energy components using the aug-cc-pVDZ basis set. Therefore, the components were estimated using an approximate procedure proposed in ref. 43, accurate enough to find the dominant components (the results thus obtained are collected in Table 5):

(a) The induction component, E_{ind}, can be discarded for being much smaller than the other components.
(b) The electrostatic component, E_{el}, was approximated as a Coulombic interaction between two multipolar distributions, further truncating the multipole expansion at first order. That is, was expressed as the sum of $-[q_i q_j]/r_{ij}$ for all unique pairs of atoms of the AB dimer, where q_i and q_j are the net charges of atoms *i* and *j*, where atom *i* belongs to molecule A, atom *j* to molecule B, and r_{ij} is the distance between the atoms *i* and *j* (CHelp q_i charges were used, obtained from MP2/aug-cc-pVDZ calculations).
(c) The dispersion term, E_{disp}, was obtained as the difference between the MP2 and HF interaction energies.
(d) The exchange-repulsion component, E_{er} (or, more appropriately, the exchange-repulsion plus induction components, (E_{er} + E_{ind})) are obtained by subtracting the previous two terms from the MP2 interaction energy.

The results in Table 5 show that dispersion component is always the dominant stabilizing term, being its value about ten times stronger than the electrostatic component. Note, in passing, that the electrostatic component only becomes numerically relevant when at least one of the θ_1 or θ_2 angles is smaller than 90º.

Table 5. Components of the interaction energy (in kcal·mol^{-1}) for the 9 dimers selected from those of Table 4 (see text for the selection procedure and the physical meaning of these components). For each dimer, the Refcode of the crystal where it is found, the Cl···Cl distance, the θ_1 and θ_2 angles, and BSSE-corrected interaction energy (computed at the MP2/aug-cc.pVDZ level, in kcal·mol^{-1}) are also given.

	r (Å)	θ_1 (º)	θ_1 (º)	E_{el}	E_{disp}	$E_{er}+E_{ind}$	$E_{int,MP2}$
CMALAM10	3.10	165.2	165.2	0.07	-2.89	2.51	-0.31
AHUMUL	3.27	150.5	135.0	0.16	-2.65	2.23	-0.26
DCHLAN01	3.32	156.1	164.6	-0.06	-2.07	1.51	-0.62
BAGCET	3.39	104.4	164.4	0.04	-2.78	1.22	-1.52
CLBZAP02	3.44	167.4	167.4	-0.01	-1.62	0.90	-0.73
CIMALI	3.49	158.2	157.9	0.01	-1.54	0.83	-0.71
CLACET01	3.55	165.8	81.5	-0.78	-1.60	1.06	-1.33
CLACET01	3.71	79.6	160.8	0.25	-1.50	0.13	-1.12
CCACEN	3.83	72.2	72.2	0.46	-2.55	0.66	-1.43

CONCLUSIONS

The nature of the C-Cl···Cl-C interactions was investigated by doing of MP2/aug-cc-pVDZ calculations on model dimers and on dimers extracted from the Cambridge Crystallographic Data Centre (CCDC). The study was divided in the following four parts: (1) analysis of the C-Cl···Cl-C interactions in CCl_4···CCl_4 dimers, oriented in hypothetical model geometries and for all unique first-nearest neighbors dimers present in the CCl_4 crystal; (2) study of the impact of the chlorination degree in n-substituted chloromethane dimers ($CH_{4-n}Cl_n$···$CH_{4-n}Cl_n$, n = 1, 2, and 3); (3) study of the impact of the C(*ipso*) hybridization on the strength of the C-Cl···Cl-C interactions; and (4) evaluation of the strength of the C-Cl···Cl-C interactions for a set of 45 dimers extracted from the crystals deposited in the CCDC, selected in such a way that their only Cl···Cl distance cover the 2.75-4 Å range in a smooth way. In order to get a quantitative insight about the nature of these C-Cl···Cl-C interactions, the evaluation of their interaction energy was complemented by: (a) a computation of its dominant energetic component (done at SAPT level, for small dimers, or using an approximate procedure reported in the literature, for large dimers), and (b) an AIM analysis (looking for the characteristic properties of the Cl···Cl bond critical point present in each dimer).

The results here obtained numerically demonstrate: (a) the higher stability of the dimer orientations where the number of short-distance Cl···Cl contacts are maximized; (b) quantify the impact of diminishing the chlorination degree of the C(*ipso*) atom in $CH_{4-n}Cl_n$···$CH_{4-n}Cl_n$, dimers, showing the creation of a dipole moment in each interacting fragment, which results in the presence of an electrostatic component in the dimer interaction energy (stabilizing only when both dipoles are properly oriented); (c) the $E(\theta_1, \theta_2)$ potential energy surface of the $(CH_3Cl)_2$ dimer presents a Type I minimum (at $\theta_1 = \theta_2 = 90º$) and two symmetry equivalent Type II minima (when either θ_1 or θ_2 is 90º and the other angle is 180º), being the $\theta_1 = \theta_2 = 155º$ Type I orientation is a saddle point between both Type II minima; (d) the dispersion component is the dominant term in all C-Cl···Cl-C interactions studied, regardless the C(*ipso*) hybridization, orientation of the C-Cl groups, or degree of chlorination; (e) MP2/CBS calculations provide reference values for the C(sp^n)-Cl···Cl-C(sp^n) interactions: -1.14, -1.29, and -1.40 kcal·mol^{-1} for C(sp^3), C(sp^2-aliphatic) and C(sp), respectively; (f) Statistically, the C-Cl···Cl-C contacts present in molecular crystals present a maximum around 3.8 Å and a preference for Type I contacts (where $\theta_1 = \theta_2$), particularly around 90º and 150º, as well as for Type II interactions placed close to their minima; (g) C-Cl···Cl-C interactions found in crystals fail to fulfill the strength-length distribution that should correlate E_{int} and the Cl···Cl distance; and (h) a previously proposed correlation between the density at the Cl···Cl bond critical point and the strength of the C-Cl···Cl-C interaction was found to fail at short Cl···Cl distances.

TABLE OF CONTENTS

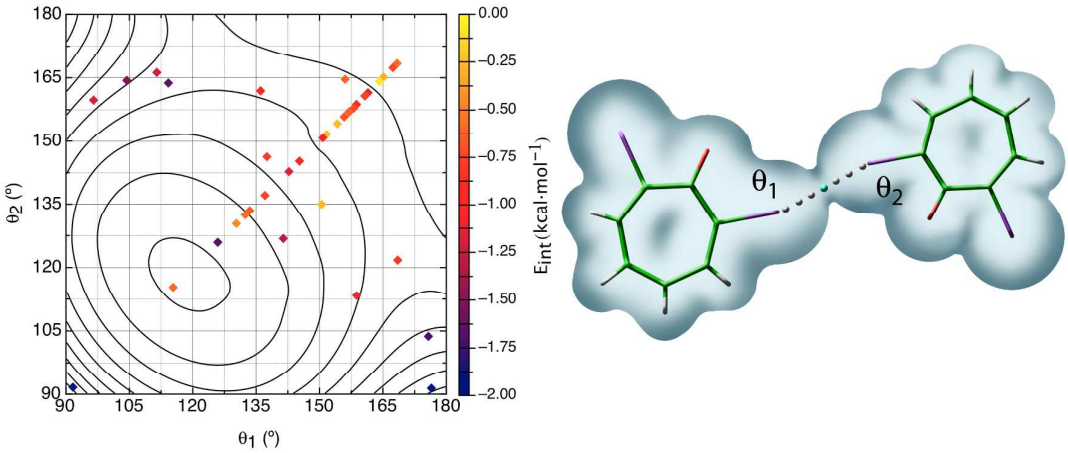

An exhaustive study of the nature of the C-Cl···Cl-C interactions found in crystals has been carried out at the MP2/aug-cc-pVDZ level, using model dimers and a set of 45 dimers, extracted from the Cambridge Crystallographic Data Centre and presenting Cl···Cl distances smoothly distributed within the 2.75 – 4 Å range.

ACKNOWLEDGEMENTS

This work was financially supported by the Spanish MINECO (MAT2011-25972) and the "Generalitat de Catalunya" (2009-SGR-1203). Thanks are also given to CESCA and BSC for generous allocation of computer time in their computers.

REFERENCES

1. K. Yamasaki, *J. Phys. Soc. Japan*, 1962, **17**, 1262–1267.
2. S. C. Nyburg, *J. Chem. Phys.*, 1964, **40**, 2493.
3. I. H. Hillier, *J. Chem. Phys.*, 1967, **46**, 3881.
4. N. Ramasubbu, R. Parthasarathy, and P. Murray-Rust, *J. Am. Chem. Soc.*, 1986, **108**, 4308–4314.
5. G. R. Desiraju and R. Parthasarathy, *J. Am. Chem. Soc.*, 1989, **111**, 8725–8726.
6. F. F. Awwadi, R. D. Willett, K. a Peterson, and B. Twamley, *Chem. Eur. J.*, 2006, **12**, 8952–8960.
7. T. T. T. Bui, S. Dahaoui, C. Lecomte, G. R. Desiraju, and E. Espinosa, *Angew. Chem. Int. Ed.*, 2009, **48**, 3838–3841.
8. J. A. R. P. Sarma and G. R. Desiraju, *Acc. Chem. Res.*, 1986, **19**, 222–228.
9. G. A. Jeffrey, *An Introduction to Hydrogen Bonding*, Oxford University Press, 1997.
10. S. Scheiner, *Hydrogen Bonding: A Theoretical Perspective*, Oxford University Press, 1997.
11. W. C. Hamilton and J. A. Ibers, *Hydrogen bonding in solids*, W. A. Benjamin, Inc., 1968.
12. P. Metrangolo, H. Neukirch, T. Pilati, and G. Resnati, *Acc. Chem. Res.*, 2005, **38**, 386–395.
13. R. B. Walsh, C. W. Padgett, P. Metrangolo, G. Resnati, T. W. Hanks, and W. T. Pennington, *Cryst. Growth Des.*, 2001, **1**, 165–175.
14. C. A. Hunter and J. K. M. Sanders, *J. Am. Chem. Soc.*, 1990, **112**, 5525–5534.
15. G. R. Desiraju and A. Gavezzotti, *J. Chem. Soc. Chem. Commun.*, 1989, 621.
16. S. Tsuzuki, K. Honda, T. Uchimaru, M. Mikami, and K. Tanabe, *J. Am. Chem. Soc.*, 2002, **124**, 104–12.
17. G. R. Desiraju, *The weak hydrogen bond in structural chemistry and biology*, Oxford University Press, 1990.
18. E. D'Oria and J. J. Novoa, *CrystEngComm*, 2008, **10**, 423.
19. D. Braga and F. Grepioni, *New J. Chem.*, 1998, **22**, 1159–1161.
20. G. R. Desiraju, *J. Chem. Sci.*, 2010, **122**, 667–675.
21. G. R. Desiraju, *J. Am. Chem. Soc.*, 2013, **135**, 9952–67.
22. D. E. Williams and L. Y. Hsu, *Acta Crystallogr. Sect. A*, 1985, **41**, 296–301.
23. S. C. Nyburg and W. Wong-Ng, *Proc. R. Soc. A Math. Phys. Eng. Sci.*, 1979, **367**, 29–45.
24. S. C. Nyburg and W. Wong-Ng, *Inorg. Chem.*, 1979, **18**, 2790–2791.
25. L. Price, A. J. Stone, J. Lucas, R. S. Rowland, and A. E. Thomleytj, *J. Am. Chem. Soc.*, 1994, **116**, 4910–4918.
26. M. V Vener, A. V Shishkina, A. A. Rykounov, and V. G. Tsirelson, *J. Phys. Chem. A*, 2013, **117**, 8459–67.

27. V. R. Hathwar and T. N. Guru Row, *J. Phys. Chem. A*, 2010, **114**, 13434–13441.

28. T. Clark, M. Hennemann, J. S. Murray, and P. Politzer, *J. Mol. Model.*, 2007, **13**, 291–296.

29. R. M. Osuna, V. Hernández, J. T. L. Navarrete, E. D'Oria, and J. J. Novoa, *Theor. Chem. Acc.*, 2010, **128**, 541–553.

30. T. Helgaker, W. Klopper, H. Koch, and J. Noga, *J. Chem. Phys.*, 1997, **106**, 9639.

31. A. Halkier, T. Helgaker, P. Jørgensen, W. Klopper, H. Koch, J. Olsen, and A. K. Wilson, *Chem. Phys. Lett.*, 1998, **286**, 243–252.

32. S. F. Boys and F. Bernardi, *Mol. Phys.*, 1970, **19**, 553–566; J. J. Novoa, M. Planas and M. H. Whangbo, *Chem. Phys. Lett.*, 1994, **225**, 240-246; J. J. Novoa, M. Planas and M. C. Rovira, *Chem. Phys. Lett.*, 1996, **251**, 33-46; J. J. Novoa and M. Planas, *Chem. Phys. Lett.*, 1998, **285**, 186-197; F. B. van Duijneveldt, J. G. C. M. van Duijneveldt-van de Rijdt and J. H. van Lenthe, *Chem. Rev.*, 1994, **94**, 1873-1885.

33. Gaussian03, RevisionE.01, M. J. Frisch, G. W. Trucks, H. B. Schlegel, G. E. Scuseria, M. A. Robb, J. R. Cheeseman, G. Scalmani, V. Barone, B. Mennucci, G. A. Petersson, H. Nakatsuji, M. Caricato, X. Li, H. P. Hratchian, A. F. Izmaylov, J. Bloino, G. Zheng, J. L. Sonnenberg, M. Hada, M. Ehara, K. Toyota, R. Fukuda, J. Hasegawa, M. Ishida, T. Nakajima, Y. Honda, O. Kitao, H. Nakai, T. Vreven, J. E. MontgomeryJ. A., Jr. Peralta, F. Ogliaro, M. Bearpark, J. J. Heyd, E. Brothers, K. N. Kudin, R. Staroverov, V. N Kobayashi, J. Normand, K. Raghavachari, A. Rendell, J. C. Burant, S. S. Iyengar, J. Tomasi, M. Cossi, N. Rega, N. J. Millam, M. Klene, J. E. Knox, J. B. Cross, V. Bakken, C. Adamo, J. Jaramillo, R. Gomperts, R. E. Stratmann, O. Yazyev, A. J. Austin, R. . Cammi, C. Pomelli, J. W. Ochterski, R. L. Martin, K. Morokuma, V. G. Zakrzewski, G. A. Voth, P. Salvador, J. J. Dannenberg, S. Dapprich, A. D. Daniels, Ö. Farkas, J. B. Foresman, J. V. Ortiz, J. Cioslowski, and D. J. Fox, Gaussian Inc., Wallingford, 2003.

34. B. Jeziors, I. Robert, and K. Szalewicz, *Chem. Rev.*, 1994, **94**, 1887–1924.

35. J. Wu, H. Yan, Y. Jin, H. Chen, G. Dai, A. Zhong, and F. Pan, *J. Mol. Struct. THEOCHEM*, 2009, **911**, 132–136.

36. SAPT2008: "An Ab Initio Program for Many-Body Symmetry-Adapted Perturbation Theory Calculations of Intermolecular Interaction Energies", R. Bukowski, W. Cencek, P. Jankowski, B. Jeziorski, M. Jeziorska, S. A. Kucharski, V. F. Lotrich, A. J. Misquitta, R. Moszynski, K. Patkowski, R. Podeszwa, S. Rybak, K. Szalewicz, H. L. Williams, R. J. Wheatley, P. E. S. Wormer, and P. S. Zuchowski.

37. R. F. W. Bader, *Atoms in Molecules: A Quantum Theory*, Oxford University Press, 1994.

38. F. W. Biegler-könig, R. F. W. Bader, and T.-H. Tang, *J. Comput. Chem.*, 1982, **3**, 317–328.

39. F. H. Allen, *Acta Crystallogr. Sect. B Struct. Sci.*, 2002, **58**, 380–388.

40. E. D'Oria and J. J. Novoa, *CrystEngComm*, 2004, **6**, 367-376; J. J. Novoa and E. D'Oria, in *Engineering of Crystalline Materials Properties: State of the Art in Modeling, Design and Applications*, eds. J. J. Novoa, D. Braga and L. Addadi, 2008, pp. 307-332; E. D'Oria, D. Braga and J. J. Novoa, *CrystEngComm*, 2012, **14**, 792-79.

41. E. Espinosa, E. Molins, and C. Lecomte, *Chem. Phys. Lett.*, 1998, **285**, 170–173.

42. I. Mata, I. Alkorta, E. Molins, and E. Espinosa, *Chem. Eur. J.*, 2010, **16**, 2442–2452.

43. F. Mota, J. S. Miller, and J. J. Novoa, *J. Am. Chem. Soc.*, 2009, **131**, 7699–7707.